International Journal of Advance Scientific Research
(ISSN – 2750-1396)
VOLUME 06 ISSUE 11 Pages: 131-140
OCLC – 1368736135



Journal Website: http://sciencebring.com/index.php/ijasr

Copyright: Original content from this work may be used under the terms of the creative commons attributes 4.0 licence.

Research Article

Autofocus and Closed-Loop Backlight Control for A Machine-Vision Knitted Fabric Inspection Station: Choice of Focus Measure, Search Strategy and Integral Gain

Submission Date: October 08, 2026, **Accepted Date:** October 29, 2026,
Published Date: November 26, 2026
Crossref doi: https://doi.org/10.37547/ijasr-06-11-09

Sherzod Korabayev
Namangan State Technical University, Namangan, Uzbekistan

Sherzod Djuraev
Namangan State Technical University, Namangan, Uzbekistan

Jakhongir Soloxiddinov
Namangan State Technical University, Namangan, Uzbekistan

Shaxlo Aripova
Tashkent Institute of Textile and Light Industry, Tashkent, Uzbekistan

Abstract

An inspection camera can only find small faults in knitted fabric if the image is sharp and its brightness stays in the range for which the detector was set. On an inspection machine, both conditions change during a shift: fabric of a different thickness moves the surface out of the depth of field, and the transmission of the fabric and the output of the LED backlight drift. This paper studies two control loops of the knitted fabric inspection station built on an ST-KFIM-01-240 machine: a servo-driven autofocus and an integral controller that sets the LED drive from the mean image brightness. Five focus measures (variance of the Laplacian, Tenengrad, Brenner gradient, normalised variance and the sum-modified Laplacian) were evaluated on backlit single-jersey texture blurred over 51 lens positions at two noise levels. All five peaked within one step of the true focus. At the higher noise level, however, the two Laplacian-based measures became multimodal (on average 2.0–2.4 local maxima) and their peak-to-background ratio fell to 1.3–1.6. Tenengrad kept a single peak with a ratio of 34. A coarse-to-fine hill-climbing search with a halving step found focus to within 0.5 step in about 10 image evaluations for every gradient-based measure, while a fixed small step stopped 16–38 steps away from focus. For the backlight, a model including the thermal

International Journal of Advance Scientific Research
(ISSN – 2750-1396)
VOLUME 06 ISSUE 11 Pages: 131-140
OCLC – 1368736135

derating of the LED and a step change in fabric transmission showed that the open-loop brightness error reached 0.18 of full scale after the change. An integral controller with gains of 0.2–0.6 per sample held the RMS error at 0.006–0.009 and recovered from the fabric change in 0.8–2.7 s. The recommended configuration is Tenengrad with adaptive hill climbing, refocusing on article change or on a drop in sharpness, and integral brightness control at a gain of about 0.5 per sample, a value well inside the stability limit of the discrete loop.

Keywords

knitted fabric inspection; machine vision; autofocus; focus measure; LED backlight; integral control; image quality.

Introduction

Automatic fabric inspection is usually discussed as a problem of image analysis, and most published work compares feature extractors, classifiers and neural networks [1]–[3]. Less attention is paid to whether the images reaching the algorithm are good enough. Two image properties matter most on an inspection table. The first is sharpness. A knitted loop on single-jersey fabric is about 1.5–2 mm high, and broken filaments, fine holes and thin places are smaller still. A small defocus blurs these details into the texture. The second is brightness. Statistical and learned detectors are set, or trained, on images with a certain grey-level distribution. If the brightness drifts, either the histogram saturates and detail is lost, or the threshold that separates faults from normal texture no longer corresponds to the same contrast.

In the inspection station developed in the project “Development of methods and algorithms for assessing the quality indicators of knitted fabrics on the basis of artificial intelligence”, the fabric passes over a table lit from behind by LEDs and is imaged by an industrial camera. A Raspberry Pi controller sets the LED drive through a digital potentiometer and moves the lens with a servo actuator, while the main computer runs the image analysis. The project report proposed closing both loops on image statistics: the mean brightness for the light and a Laplacian sharpness function for the focus. It also noted that the three subsystems of the station have very different speeds, with the light being the fastest, the focus intermediate and the fabric transport the slowest. This paper makes those proposals concrete. It answers three questions. Which focus measure is reliable on backlit knitted texture, and is the Laplacian a good choice? How should the focus search be organised? What integral gain gives fast and stable brightness control under realistic drifts?

Focus measures have been compared many times, for microscopy [4], for general imaging [5]–[7] and for shape from focus [8], [9]. These studies

International Journal of Advance Scientific Research
(ISSN – 2750-1396)
VOLUME 06 ISSUE 11 Pages: 131-140
OCLC – 1368736135

agree that gradient-based and Laplacian-based measures are the most discriminating, but they disagree on noise robustness, which depends on the image content. A knitted fabric is a strongly periodic texture with high contrast at a known spatial frequency. Its behaviour cannot be taken for granted from results on cells or natural scenes. Climbing searches with adaptive steps are standard in camera autofocus [10]. LED output is known to fall as junction temperature rises [11], and fabric transmission varies with areal density and structure. Together, these effects make open-loop lighting unsuitable for a station that has to work through a shift on different articles. Software contrast correction, such as adaptive histogram equalisation [9], can only partly compensate, because it amplifies noise and changes the texture statistics on which the detector relies. Image-quality control at the source also supports the digital-twin quality model of the production line developed earlier by the team [12], which assumes that the inspection data are comparable over time.

MODELS

1. Focus measures

Let I(x, y) be an image window. The five measures examined are:

$$F_{LV} = \mathrm{Var}[\nabla^2 I], \qquad F_T = \overline{G_x^2 + G_y^2} \qquad (1)$$

$$F_B = \overline{[I(x+2,y) - I(x,y)]^2}, \qquad F_{NV} = \frac{\mathrm{Var}(I)}{\bar{I}} \qquad (2)$$

$$F_{SML} = \overline{|2I(x,y) - I(x-1,y) - I(x+1,y)| + |2I(x,y) - I(x,y-1) - I(x,y+1)|} \qquad (3)$$

Here ∇^2 is the discrete Laplacian, G_x and G_y are Sobel gradients, and the bar denotes the mean over the window. F_{LV} is the variance of the Laplacian, F_T the Tenengrad, F_B the Brenner gradient [4], F_{NV} the normalised variance [4], [5] and F_{SML} the sum-modified Laplacian [8]. The Laplacian sharpness function proposed in the project report corresponds to F_{LV}.

2. Defocus

Within the depth of field, the defocus point-spread function of the lens is approximated by a Gaussian whose width grows linearly with the distance of the lens from the best-focus position z*:

$$I_z = G_{\sigma(z)} * I_0 + n, \qquad \sigma(z) = c|z - z^*| + \sigma_0 \qquad (4)$$

where I0 is the sharp image, n is sensor noise, c = 0.08 pixel per actuator step and σ0 = 0.3 pixel. The actuator range is 0–100 steps and z* = 55. With these values, the blur at the ends of the range is 3.7–4.7 pixels, about one-quarter of a stitch cell at 0.125 mm/pixel.

3. Brightness model and integral control

Let u ∈ [0, 1] be the normalised LED drive. The mean image brightness at sample k is

International Journal of Advance Scientific Research
(ISSN – 2750-1396)
VOLUME 06 ISSUE 11 Pages: 131-140
OCLC – 1368736135

$$B_k = G\,T_k\,\eta(\vartheta_k)\,u_k + e_k, \qquad \eta(\vartheta) = 1 - \beta(\vartheta - \vartheta_0) \qquad (5)$$

where G is the optical gain of the table and camera, T_k the fabric transmission, e_k measurement noise, and η the relative LED output, which falls with the junction temperature ϑ at a rate β [11]. The junction temperature follows a first-order thermal model:

$$\vartheta_{k+1} = \vartheta_k + \frac{T_s}{\tau_{th}}(\vartheta_0 + \Delta\vartheta_{max}u_k - \vartheta_k) \qquad (6)$$

The controller is a discrete integrator acting on the brightness error:

$$u_{k+1} = \mathrm{sat}_{[0,1]}[u_k + K_i(B^* - B_k)] \qquad (7)$$

Ignoring the slow thermal term, the loop gain is $\lambda = K_i G T \eta$, and the closed loop $e_{k+1} = (1 - \lambda)e_k$ is stable for $0 < \lambda < 2$. It is fastest and without overshoot for $\lambda = 1$ [13]. Because T changes from article to article, K_i should be chosen so that λ stays well below 2 for the most transparent fabric. The values used in the simulation were $G = 2.4$, $\beta = 0.4\%/\mathrm{K}$, $\vartheta_0 = 25\ ^\circ\mathrm{C}$, $\Delta\vartheta_{max} = 55\ \mathrm{K}$, $\tau_{th} = 60\ \mathrm{s}$, $T_s = 0.1\ \mathrm{s}$, and a set point $B^* = 0.5$ (128 of 255 grey levels). The fabric transmission was 0.42 for the first 120 s and then 0.30, representing a change from a lighter to a heavier article. A 3% periodic variation with a 7 s period was superimposed to represent changes in density along the roll.

Methods

1. Images

A sharp backlit single-jersey image (256 × 256 pixels, stitch cell of 16 × 12 pixels, about 2.0 × 1.5 mm) was generated with the same synthetic model used in the companion study on defect segmentation. In this model, two inclined loop legs per cell carry random amplitude variation and the transmission is an exponential function of yarn density. The image was blurred according to Eq. (4) at lens positions 0, 2, …, 100 (51 positions), and Gaussian noise with a standard deviation of 0.01 or 0.04 of full scale was added. Each focus curve was computed five times with independent noise.

2. Indicators of a good focus measure

For each curve, four indicators were computed: (i) the error of the peak position, |zpeak − z*|; (ii) the width of the curve at 50% of its normalised height (a narrower curve is more precise but harder to find from far away); (iii) the number of local maxima above 5% of the normalised height (the ideal value is one); and (iv) the ratio of the peak value to the value at the far end of the range, which shows how strongly the measure separates focused from defocused images.

3. Search strategies

Two searches were compared, each started from four positions (5, 20, 80, 95). The fixed-step search moves in steps of 2 and stops at the first decrease. The adaptive search starts with a step of 16, and at each decrease halves the step and reverses direction until the step reaches 1, following the logic of coarse-to-fine climbing

International Journal of Advance Scientific Research
(ISSN – 2750-1396)
VOLUME 06 ISSUE 11 Pages: 131-140
OCLC – 1368736135

searches [10]. The result is the final position error and the number of image evaluations, each of which costs one frame.

4. Brightness control

Equations (5)–(7) were simulated for 300 s (3,000 samples) in open loop (u constant at the value that gives B* on the first fabric) and with Ki = 0.2 and 0.6, giving λ ≈ 0.18 and 0.54 on the first fabric. The RMS and maximum brightness errors, the mean absolute error 10–30 s after the fabric change, the time to return within 1% of the set point, the final junction temperature and the final drive were recorded.

Results

1. Focus curves

Figure 1 shows normalised focus curves at the two noise levels, and Table 1 gives the indicators.

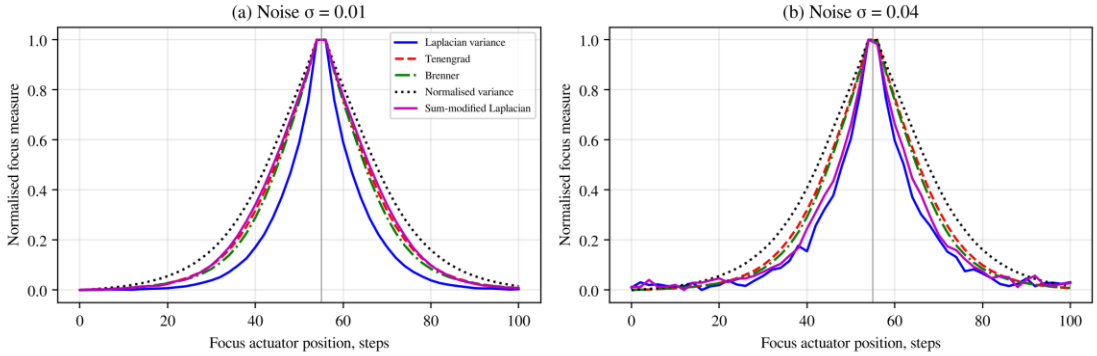


Figure 1. Normalised focus measures as functions of the lens position for backlit single-jersey texture: (a) noise SD 0.01; (b) noise SD 0.04. The vertical line marks the true focus

Table 1. Indicators of the focus measures (means of five noise realisations)

Focus measure	Peak error, steps (0.01 / 0.04)	Width at 50%, steps (0.01 / 0.04)	Local maxima (0.01 / 0.04)	Peak/far-end ratio (0.01 / 0.04)
Variance of Laplacian	1 / 1	10 / 10	1.0 / 2.4	11.4 / 1.6
Tenengrad	1 / 1	18 / 18	1.0 / 1.0	215 / 34
Brenner	1 / 1	18 / 18	1.0 / 1.0	134 / 17
Normalised variance	1 / 1	22 / 22	1.0 / 1.0	82 / 27
Sum-modified Laplacian	1 / 1	18 / 14	1.0 / 2.0	3.5 / 1.3

International Journal of Advance Scientific Research
(ISSN – 2750-1396)
VOLUME 06 ISSUE 11 Pages: 131-140
OCLC – 1368736135

Crossref doi Google Scholar WorldCat MENDELEY

ISSN-2750-1396

All five measures placed their maximum within one step of the true focus. The differences lie in the shape of the curves. The two Laplacian-based measures had the narrowest peaks, but they were also the most sensitive to noise. The Laplacian is a second-difference operator and amplifies pixel noise. When the image is defocused, the texture contribution to the Laplacian falls, while the noise contribution does not. At the higher noise level, the variance of the Laplacian therefore stayed almost as high far from focus as at focus (ratio 1.6), and its curve developed on average 2.4 local maxima. The sum-modified Laplacian behaved similarly. The first-order gradient measures (Tenengrad and Brenner) and the normalised variance kept a single maximum and a large ratio at both noise levels. Tenengrad gave the largest ratio, 215 and 34, because the Sobel operator smooths across the gradient direction and so suppresses part of the noise.

2. Focus search

Table 2 gives the search results.

Table 2. Autofocus search: mean final error (steps) and number of image evaluations, averaged over four starting positions

Focus measure	Noise	Adaptive: error / evaluations	Fixed step 2: error / evaluations
Variance of Laplacian	0.01	0.25 / 10.5	29.0 / 6.5
	0.04	24.0 / 7.0	37.0 / 2.8
Tenengrad	0.01	0.25 / 10.5	16.5 / 12.5
	0.04	0.50 / 10.0	16.5 / 12.5
Brenner	0.01	0.50 / 10.0	16.5 / 12.8
	0.04	0.25 / 10.5	16.5 / 12.8
Normalised variance	0.01	0.00 / 11.0	16.5 / 12.8
	0.04	0.25 / 10.5	16.5 / 12.5
Sum-modified Laplacian	0.01	0.25 / 10.5	29.0 / 6.3
	0.04	0.50 / 10.0	37.5 / 3.0

The fixed small step failed in every case. Starting far from focus, the curve is flat, and a step of 2 produces a change smaller than the noise, so the search stops on the first random decrease. The adaptive search took large steps first, where the curve is flat, and small steps near the peak, where it is steep. With every gradient-based measure, it reached focus to within half a step in 10–11 evaluations at both noise levels. With the variance of the Laplacian at the higher noise level, the adaptive search also failed (mean error 24 steps), because its curve had secondary maxima at which the search could stop. At four frames per second, the frame rate needed at the highest fabric speed, 10–11 evaluations take about 2.5 s. With a faster dedicated acquisition during refocusing (60 frames per second is available on the station camera), the search takes about 0.2 s.

International Journal of Advance Scientific Research
(ISSN – 2750-1396)
VOLUME 06 ISSUE 11 Pages: 131-140
OCLC – 1368736135

3. Brightness control

Figure 2 shows the brightness and the LED drive, and Table 3 summarises the results.

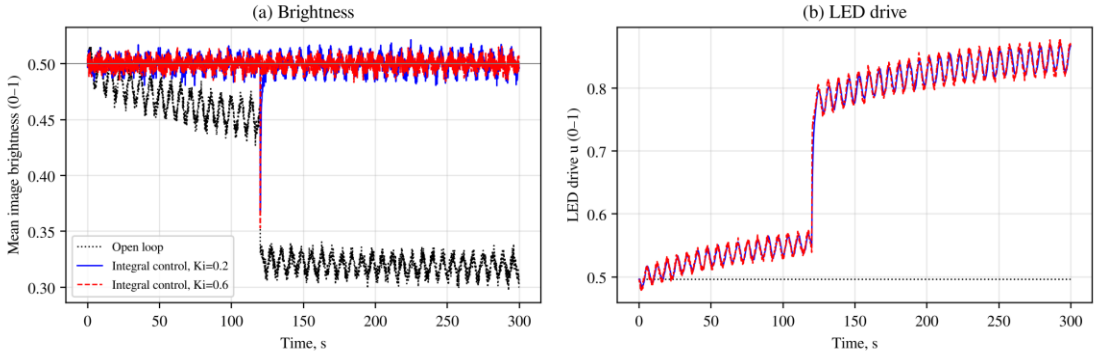


Figure 2. Mean image brightness (a) and LED drive (b) in open loop and under integral control. The fabric transmission falls from 0.42 to 0.30 at t = 120 s

Table 3. Brightness control performance (brightness on a 0–1 scale, set point 0.5)

Mode	RMS error	Max error	Mean abs. error 10–30 s after change	Recovery to 1%, s	Final junction temp., °C	Final drive
Open loop	0.143	0.203	0.178	—	52.1	0.50
Integral, K_i = 0.2	0.0088	0.133	0.0061	2.7	70.0	0.87
Integral, K_i = 0.6	0.0061	0.147	0.0038	0.8	70.0	0.86

In open loop, the brightness first fell slowly as the LEDs warmed up (by about 11% over the first two minutes) and then fell sharply when the heavier fabric arrived. The mean error after the change was 0.178 of full scale, about 45 grey levels. Both integral controllers held the brightness close to the set point. The maximum errors of 0.13–0.15 in Table 3 occur at the instant of the fabric change and last only a few samples. The higher gain recovered from the change in 0.8 s and the lower gain in 2.7 s. The periodic density variation was also largely removed, more completely at the higher gain. The cost of control is a higher drive, 0.86–0.87 instead of 0.50, needed to compensate for the darker fabric and the thermal derating. The higher drive in turn raises the junction temperature to about 70 °C, which reduces LED efficiency and lifetime. This shows that the light source should have a margin: in this example, the controller used 87% of the available drive, leaving little reserve for a still heavier fabric.

Discussion

The focus results lead to a clear recommendation that differs from the initial proposal in the project

International Journal of Advance Scientific Research
(ISSN – 2750-1396)
VOLUME 06 ISSUE 11 Pages: 131-140
OCLC – 1368736135

report. The variance of the Laplacian is a sound measure in clean images and has the narrowest peak, but on backlit knitted fabric with realistic sensor noise it becomes multimodal. A climbing search can then stop at a false maximum. Tenengrad keeps a single, high peak at both noise levels and costs no more to compute. If the Laplacian is preferred for its sharper peak, the image should be smoothed before the Laplacian is applied, or the Laplacian should be used only in the last, fine stage of the search, after a gradient measure has brought the lens close to focus. This agrees with the observation in comparative studies that noise robustness, not peak width, usually decides the choice of focus measure in practical systems [5], [6].

The search strategy matters as much as the measure. A fixed small step is unsuitable on texture whose focus curve is flat far from focus. The coarse-to-fine search reached focus in about ten frames, which is short enough to repeat whenever needed. Refocusing does not have to run continuously. The station knows when a new article starts, and the focus measure is already computed for every inspection frame. A practical rule is therefore to refocus at each article change and whenever the running mean of the focus measure falls below a set fraction (for example, 70%) of its value just after the last refocus. This matches the intermediate position of the focus actuator in the speed hierarchy of the station noted in the project report.

For the light, the analysis of Eq. (7) gives a simple rule for the gain. The loop gain $\lambda = KiGT\eta$ is proportional to the fabric transmission. If the gain is set for an average fabric with $\lambda \approx 0.5$, a fabric twice as transparent gives $\lambda \approx 1$, which is still stable and without overshoot, and only a fabric four times as transparent approaches the stability limit of 2. A gain of 0.5–0.6 per sample, as in the simulated case, is therefore a reasonable default. If the station is used on fabrics with very different transmissions, the gain can be scheduled by dividing it by the drive value of the previous article, which is a direct estimate of $1/(GT\eta)$. Because the light loop is about ten times faster than the fabric changes that disturb it, it can be closed on every frame without interacting with the focus loop. The focus measure itself depends on brightness, however. The focus search should therefore be run only after the brightness loop has settled, and the focus measure should be normalised by the mean brightness.

The study has limitations. Defocus was modelled as Gaussian blur, which is a good approximation near focus but not for strongly defocused lenses with a disc-shaped point-spread function. The noise was white, whereas real sensors have signal-dependent shot noise. The thermal and transmission parameters were typical rather than measured on the station. The next step is to record focus sweeps and brightness logs on the ST-KFIM-01-240 station with several articles, fit the parameters c, G, β and τ_{th}, and repeat the comparison on real images.

Conclusion

On backlit knitted fabric, all five focus measures located the true focus within one actuator step, but the Laplacian-based measures became

International Journal of Advance Scientific Research
(ISSN – 2750-1396)
VOLUME 06 ISSUE 11 Pages: 131-140
OCLC – 1368736135

multimodal at realistic noise levels. Tenengrad kept a single peak with a peak-to-background ratio of 34–215 and is recommended.

An adaptive coarse-to-fine climbing search reached focus within half a step in 10–11 frames with every gradient-based measure, while a fixed small step stopped 16–38 steps from focus. Refocusing should be triggered by article changes and by a fall in the running focus measure.

Open-loop LED lighting gave brightness errors of up to 0.18 of full scale under realistic LED warm-up and fabric changes. An integral controller with a gain of 0.2–0.6 per sample reduced the RMS error to 0.006–0.009 and recovered from a fabric change in 0.8–2.7 s.

The loop gain of the brightness controller is proportional to the fabric transmission. A gain giving $\lambda \approx 0.5$ on an average fabric keeps the loop stable over a fourfold range of transmission, and the light source should be sized so that the controller does not run close to full drive.

REFERENCES

1. Kumar, A. (2008). Computer-vision-based fabric defect detection: A survey. IEEE Transactions on Industrial Electronics, 55(1), 348–363. https://doi.org/10.1109/TIE.2007.896476
2. Ngan, H. Y. T., Pang, G. K. H., & Yung, N. H. C. (2011). Automated fabric defect detection—A review. Image and Vision Computing, 29(7), 442–458. https://doi.org/10.1016/j.imavis.2011.02.002
3. Rasheed, A., Zafar, B., Rasheed, A., Ali, N., Sajid, M., Dar, S. H., Habib, U., Shehryar, T., & Mahmood, M. T. (2020). Fabric defect detection using computer vision techniques: A comprehensive review. Mathematical Problems in Engineering, 2020, Article 8189403. https://doi.org/10.1155/2020/8189403
4. Groen, F. C. A., Young, I. T., & Ligthart, G. (1985). A comparison of different focus functions for use in autofocus algorithms. Cytometry, 6(2), 81–91. https://doi.org/10.1002/cyto.990060202
5. Krotkov, E. (1988). Focusing. International Journal of Computer Vision, 1(3), 223–237. https://doi.org/10.1007/BF00127822
6. Subbarao, M., & Tyan, J.-K. (1998). Selecting the optimal focus measure for autofocusing and depth-from-focus. IEEE Transactions on Pattern Analysis and Machine Intelligence, 20(8), 864–870. https://doi.org/10.1109/34.709612
7. Pertuz, S., Puig, D., & Garcia, M. A. (2013). Analysis of focus measure operators for shape-from-focus. Pattern Recognition, 46(5), 1415–1432. https://doi.org/10.1016/j.patcog.2012.11.011
8. Nayar, S. K., & Nakagawa, Y. (1994). Shape from focus. IEEE Transactions on Pattern Analysis and Machine Intelligence, 16(8),

International Journal of Advance Scientific Research
(ISSN – 2750-1396)
VOLUME 06 ISSUE 11 Pages: 131-140
OCLC – 1368736135

824–831. https://doi.org/10.1109/34.308479

9. Pizer, S. M., Amburn, E. P., Austin, J. D., Cromartie, R., Geselowitz, A., Greer, T., ter Haar Romeny, B., Zimmerman, J. B., & Zuiderveld, K. (1987). Adaptive histogram equalization and its variations. Computer Vision, Graphics, and Image Processing, 39(3), 355–368. https://doi.org/10.1016/S0734-189X(87)80186-X

10. He, J., Zhou, R., & Hong, Z. (2003). Modified fast climbing search auto-focus algorithm with adaptive step size searching technique for digital camera. IEEE Transactions on Consumer Electronics, 49(2), 257–262. https://doi.org/10.1109/TCE.2003.1209511

11. Schubert, E. F. (2006). Light-emitting diodes (2nd ed.). Cambridge University Press. https://doi.org/10.1017/CBO9780511790546

12. Korabayev, S., Bobojanov, X., Soloxiddinov, J., Inomov, Z., & Boltabayev, S. (2026). Hybrid modeling and digital twin integration for predictive quality control and resource optimization in smart knitted fabric manufacturing. The American Journal of Engineering and Technology, 8(1), 201–211. https://doi.org/10.37547/tajet/Volume08Issue01-19

13. Åström, K. J., & Murray, R. M. (2021). Feedback systems: An introduction for scientists and engineers (2nd ed.). Princeton University Press.